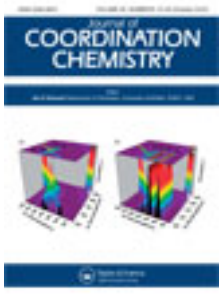

Journal of Coordination Chemistry
Publication details, including instructions for authors and subscription information:
http://www.tandfonline.com/loi/gcoo20

Synthesis, structure, DNA-binding, and nuclease activity of a 3d-4f mixed metal nitrosyl complex, $[Pr(phen)_2(MeOH)(H_2O)_2][Fe(CN)_5(NO)]\cdot(Phen)(DMF)(MeOH)(H_2O)$

Sujoy Roy Chowdhury [a], MD. Selim [a], Suparna Chatterjee [a], Satoshi Igarashi [b], Yasuhiko Yukawa [b] & Kalyan K. Mukherjea [a]
[a] Department of Chemistry, Jadavpur University, Kolkata-700032, India
[b] Graduate School of Science and Technology, Niigata University, 8050 Ikarashi-Ninocho, Niigata 950-2181, Japan
Accepted author version posted online: 03 Aug 2012.Published online: 20 Aug 2012.

To cite this article: Sujoy Roy Chowdhury, MD. Selim, Suparna Chatterjee, Satoshi Igarashi, Yasuhiko Yukawa & Kalyan K. Mukherjea (2012) Synthesis, structure, DNA-binding, and nuclease activity of a 3d-4f mixed metal nitrosyl complex, $[Pr(phen)_2(MeOH)(H_2O)_2][Fe(CN)_5(NO)]\cdot(Phen)(DMF)(MeOH)(H_2O)$, Journal of Coordination Chemistry, 65:19, 3469-3480, DOI: 10.1080/00958972.2012.718075

To link to this article: http://dx.doi.org/10.1080/00958972.2012.718075

Journal of Coordination Chemistry
Vol. 65, No. 19, 10 October 2012, 3469–3480

Synthesis, structure, DNA-binding, and nuclease activity of a 3d–4f mixed metal nitrosyl complex, $[Pr(phen)_2(MeOH)(H_2O)_2][Fe(CN)_5(NO)]\cdot(Phen)(DMF)(MeOH)(H_2O)$

SUJOY ROY CHOWDHURY†§, MD. SELIM†§, SUPARNA CHATTERJEE†, SATOSHI IGARASHI‡, YASUHIKO YUKAWA‡ and KALYAN K. MUKHERJEA*†

†Department of Chemistry, Jadavpur University, Kolkata-700032, India
‡Graduate School of Science and Technology, Niigata University, 8050 Ikarashi-Ninocho, Niigata 950-2181, Japan

(*Received 28 April 2012; in final form 6 July 2012*)

A cyano-bridged heterometallic lanthanide-transition metal nitrosyl complex, $[Pr(phen)_2(MeOH)(H_2O)_2][Fe(CN)_5(NO)]\cdot(Phen)(DMF)(MeOH)(H_2O)$ (Phen = 1,10-phenanthroline and DMF = dimethylformamide), has been synthesized from reaction of $PrCl_3\cdot 6H_2O$ with 1,10-phenanthroline in methanol and sodium nitroprusside followed by crystallization from DMF. The crystal structure shows that the complex is a 1-D chain, stabilized by coordination, hydrogen-bonding, and π–π stacking interactions. The complex shows nuclease activity with pUC19 supercoiled DNA in DMF/Tris-HCl buffer in the presence of H_2O_2.

Keywords: 3 d–4f Heterometallic complex; Cyanide-bridged complexes; π–π Stacking interactions; Metal nitrosyl compound; Nuclease activity

1. Introduction

Synthesis and study of a variety of transition metal nitrosyl complexes [1, 2] have been of interest for decades. The recent discovery of the key role of nitric oxide in human cardiovascular and nervous systems, as well as in the immune response to pathogen invasion, has revolutionized research of transition metal nitrosyl complexes [3]. Attention is now focused on the synthetic, structural, and spectroscopic properties of transition metal nitrosyl complexes along with reactivity of the coordinated NO. Reactions of coordinated nitrosyl have use in environmental, catalytic, and biochemical domains. The chemistry of transition-metal-NO complexes, or metal nitrosyls, has taken on added significance because of the important role played by nitric oxide as a

*Corresponding author. Email: k_mukherjea@yahoo.com
§Contributed equally to this work.

ISSN 0095-8972 print/ISSN 1029-0389 online
http://dx.doi.org/10.1080/00958972.2012.718075

signaling molecule in biological systems [4, 5]. NO is involved in a wide range of physiological functions, vasodilatations, inhibition of platelet aggregation, neurotransmission, and penile erection together with having a major role to play in operation of the immune system. Review articles [6–8] by biologists, biochemists, medical scientists and pharmacologists have been published on chemistry of nitric oxide, within the context of its range of biological activities. Design of small complexes that bind at specific sequences of DNA [9, 10] becomes important as we begin to delineate, on a molecular level, how genetic information is expressed. A more complete understanding of how to target DNA sites with specificity will lead not only to design of novel chemotherapeutics but also help chemists and biologists to probe DNA and to develop highly sensitive diagnostic agents. Since 1,10-phenanthroline (Phen) possesses a rigid planar aromatic ring, it has been used as a DNA intercalator [11]. Some metal complexes containing 1,10-phenanthroline are also known to bind DNA by intercalation [12, 13]; some are used to break the DNA chain in the presence of H_2O_2 [14–16]. The presence of organic rings close to the metal site plays an important role in binding the complex to DNA. So, we have synthesized and characterized structurally complexes with similar ligands which facilitate nicking of pUC19 plasmid DNA [17–19]. The present communication is an attempt to synthesize a metal nitrosyl complex and thoroughly study the interaction of the complex with DNA with a view to develop potential DNA nucleases.

2. Experimental

2.1. *Materials and general methods*

All materials and solvents were purchased commercially and used as supplied, unless otherwise mentioned. Analytical grade solvents used for physico-chemical studies were further purified by literature methods [20] before use. Solutions of CT DNA in Tris-HCl/NaCl (pH = 7.2) buffer gave a ratio of UV absorbance at 260 and 280 nm, A_{260}/A_{280}, of *ca* 1.8–1.9, indicating that the DNA was sufficiently free from protein contamination [21]. The DNA concentration was determined by absorption spectroscopy following the literature method [22]. Stock solutions were stored at 4°C and used within 4 days.

2.2. *Instrumentation*

FTIR spectra were recorded at room temperature on a Perkin Elmer RFX-I spectrophotometer from 300 to 4000 cm^{-1} in KBr pellets. UV-Vis spectra (200–900 nm) were recorded at room temperature with a Shimadzu 1601-PC Spectrophotometer using 1-cm quartz cell against appropriate reagent blank. Fluorescence emission intensity measurements were carried out using a JASCO FP 6500 Spectroflourimeter. DNA cleavage activity of the complex was monitored with the help of a Gel electrophoresis Model No. 2101, Genei, Bangalore and assessed by Gel Documentation set up.

2.3. *Preparation and characterization of the complex*

The compound was synthesized by mixing an aqueous solution (10 mL) of $Na_2[Fe(CN)_5NO]\cdot 2H_2O$ (0.30 g, 1.0 mmol) with a 10 mL aqueous solution of $PrCl_3\cdot 6H_2O$ (0.355 g, 1.0 mmol) and adding the resulting solution to 10 mL of methanolic solution of 1,10-phenanthroline monohydrate (0.79 g, 4.0 mmol). The precipitate obtained was then crystallized from DMF. After 6–7 days pale red diffraction grade crystals were obtained. The elemental analysis calculated for $C_{46}H_{45}FeN_{13}O_7Pr$ (%): Calcd C, 50.75; H, 4.17; N, 16.72. Found(%): C, 50.95; H, 4.05; N, 16.85. IR [selected bands] (KBr, cm^{-1}) 3421 [ν(OH)], 2152 [ν(CNb)], 2131 [ν(CN)t], 1918 [ν(NO)], 415 [ν(Fe–C)]. λ_{max} (nm $(mol\,L^{-1})^{-1}\,cm^{-1}$): 324 (1574), 446 (sh), 471 (sh), 483 (sh).

2.4. *X-ray crystal structure determination*

Suitable single crystal was diffracted on a Rigaku RAXIS-IV Imaging Plate diffractometer with graphite monochromated Mo-Kα radiation at 296 K. Crystallographic data and details of structure determination are summarized in tables 1–3. The data were processed with SAINT and absorption corrections were made with SADABS [23]. The structure was solved by direct and Fourier methods and refined by full-matrix least-squares on F^2 using WINGX software, which utilizes SHELX-97 [24]. For the structure solution and refinement, SHELXTL software package was used. Non-hydrogen atoms were refined anisotropically, while hydrogen atoms were placed with fixed thermal parameters at idealized positions.

2.5. *DNA-binding studies*

2.5.1. DNA-binding by UV-Vis. Absorption titration experiments were performed by maintaining the complex concentration at 45 μmol L^{-1} while varying the concentration of CT DNA from 25 to 350 μmol L^{-1}. While measuring the absorption spectra, equal quantity of CT DNA was added to both the complex solution and the reference solution to eliminate absorbance of DNA itself. From the absorption data, the intrinsic binding constant K_b was determined from a plot of [DNA]/($\varepsilon_a - \varepsilon_f$) *versus* [DNA] using the following equation [25]:

$$[DNA]/(\varepsilon_a - \varepsilon_f) = [DNA]/(\varepsilon_b - \varepsilon_f) + 1/K_b(\varepsilon_b - \varepsilon_f),$$

where [DNA] is the concentration of DNA in base pairs. The apparent absorption coefficients ε_a, ε_f, and ε_b correspond to A_{obsd}/[complex], the extinction coefficient for the free complex and extinction coefficient for the complex in the fully bound form, respectively. Plots of [DNA]/($\varepsilon_a - \varepsilon_f$) *versus* [DNA] gave a slope $1/(\varepsilon_b - \varepsilon_f)$ with intercept $1/K_b$ ($\varepsilon_b - \varepsilon_f$); K_b is obtained from slope to intercept ratio.

2.5.2. DNA-binding by fluorescence spectroscopy. CT DNA (60 μL, 125 μmol L^{-1}) solution in Tris-HCl/NaCl buffer (pH 7.2) was added to a 2.0 mL of ethidium bromide (EB) (12.5 μmol L^{-1}) in the same buffer medium to get the maximum

Table 1. Crystal data and structure refinement parameters for the complex.

Empirical formula	$C_{46}H_{45}FeN_{13}O_7Pr$
Formula weight	1088.70
Temperature (K)	296(2)
Wavelength (Å)	0.7107
Crystal system	Monoclinic
Space group	$P\ 1\ 21/c\ 1$
Unit cell dimensions (Å, °)	
a	14.2980(4)
b	13.8431(4)
c	23.3941(8)
α	90.00
β	101.735(2)
γ	90.00
Volume (Å^3), Z	4533.6(2), 4
Calculated density (g cm^{-3})	1.595
Absorption coefficient (mm^{-1})	1.446
Crystal size (mm^3)	$0.30 \times 0.18 \times 0.10$
θ range for data collection (°)	0.9–30.03
Reflections collected	39,182
Independent reflection	30.03 [$R_{(int)} = 0.050$]
Completeness to $\theta = \theta_{max}$ (%)	94.57
Refinement method	Full-matrix least-squares on F^2
Data/parameters	12,533/614
Goodness-of-fit on F^2	1.476
Final R indices [$I > 2\sigma(I)$]	$R_1 = 0.0748$, $wR_2 = 0.2018$
Largest diff. peak hole (e Å^{-3})	2.87 and −2.53

Table 2. Selected bond lengths (Å) for the complex.

Pr–O(2)	2.503(4)	Pr–N(11)	2.730(4)
Pr–O(3)	2.500(4)	Fe–N(1)	1.623(5)
Pr–O(4)	2.781(7)	N(1)–O(1)	1.163(7)
Pr–N(2)	2.617(5)	Fe–C(1)	1.938(6)
Pr–N(3)	2.635(5)	Fe–C(2)	1.950(6)
Pr–N(8)	2.720(5)	Fe–C(3)	1.943(6)
Pr–N(9)	2.718(5)	Fe–C(4)	1.938(6)
Pr–N(10)	2.720(5)	Fe–C(5)	1.939(6)

fluorescence intensity. Aliquots of 1.0 mmol L^{-1} stock solution of the complex in DMF were added to the EB bound CT DNA solution and fluorescence was measured after each addition.

2.5.3. DNA cleavage by gel electrophoresis. The supercoiled pUC19 DNA (6 μL, ~500 ng) in Tris-HCl buffer (50 mmol L^{-1}, pH 7.2) containing 50 mmol L^{-1} NaCl (2 μL) was treated with the metal complex (2 μL, 40 μmol L^{-1}) and H_2O_2 (2 μL, 50 mmol L^{-1}) followed by dilution with Tris-HCl buffer to a total volume of 20 μL. The samples were then incubated for an hour at 37°C, loading buffer containing 25% bromophenol blue, 30% glycerol (3 μL) was added and loaded on 0.8% agarose gel containing 1.0 μg m L^{-1} EB. Electrophoresis was carried out at 40 V for 2 h in TAE buffer (40 mmol L^{-1} Tris, 20 mmol L^{-1} acetic acid, 1 mmol L^{-1} EDTA, pH 7.2).

Table 3. Selected bond angles (°) for the complex.

O(2)–Pr–O(3)	137.3(1)	N(3)–Pr–N(8)	69.9(1)
O(2)–Pr–O(4)	75.5(1)	N(3)–Pr–N(9)	108.3(2)
O(2)–Pr–N(2)	72.3(2)	N(3)–Pr–N(10)	73.3(2)
O(2)–Pr–N(3)	137.4(2)	N(3)–Pr–N(11)	116.4(2)
O(2)–Pr–N(8)	74.3(1)	N(8)–Pr–N(9)	60.6(1)
O(2)–Pr–N(9)	71.5(1)	N(8)–Pr–N(10)	142.9(1)
O(2)–Pr–N(10)	135.4(1)	N(8)–Pr–N(11)	135.4(1)
O(2)–Pr–N(11)	75.4(1)	N(9)–Pr–N(10)	139.2(1)
O(3)–Pr–O(4)	78.6(2)	N(9)–Pr–N(11)	135.2(1)
O(3)–Pr–N(2)	148.2(2)	N(10)–Pr–N(11)	60.3(1)
O(3)–Pr–N(3)	72.5(2)	N(1)–Fe–C(1)	96.2(3)
O(3)–Pr–N(8)	100.3(2)	N(1)–Fe–C(2)	90.6(3)
O(3)–Pr–N(9)	69.4(1)	N(1)–Fe–C(3)	178.1(3)
O(3)–Pr–N(10)	72.7(1)	N(1)–Fe–C(4)	94.0(3)
O(3)–Pr–N(11)	124.2(1)	N(1)–Fe–C(5)	96.2(3)
O(4)–Pr–N(2)	129.1(2)	C(1)–Fe–C(2)	172.9(3)
O(4)–Pr–N(3)	146.9(2)	C(1)–Fe–C(3)	84.8(2)
O(4)–Pr–N(8)	132.3(1)	C(1)–Fe–C(4)	89.7(2)
O(4)–Pr–N(9)	75.2(1)	C(1)–Fe–C(5)	89.5(3)
O(4)–Pr–N(10)	83.1(1)	C(2)–Fe–C(3)	88.5(2)
O(4)–Pr–N(11)	67.9(1)	C(2)–Fe–C(4)	91.6(2)
N(2)–Pr–N(3)	76.1(2)	C(2)–Fe–C(5)	88.0(2)
N(2)–Pr–N(8)	73.5(2)	C(3)–Fe–C(4)	84.3(3)
N(2)–Pr–N(9)	127.2(2)	C(3)–Fe–C(5)	85.5(3)
N(2)–Pr–N(10)	93.3(2)	C(4)–Fe–C(5)	169.8(3)
N(2)–Pr–N(11)	66.5(2)		

Bands were visualized by UV light and photographed in UV tech Gel Documentation set up.

3. Results and discussion

3.1. *Structural characterization of the complex*

3.1.1. Single-crystal X-ray diffraction. The structure of $[Pr(phen)_2(MeOH)(H_2O)_2][Fe(CN)_5(NO)]$ is shown in figure 1. The iron in $[Fe(NO)(CN)_5]^{3-}$ is coordinated to five CN^- ions and one nitrogen atom of NO in an octahedral environment. The coordination number of Pr^{3+} in $[Pr(phen)_2(MeOH)(H_2O)_2]^{3+}$ is nine, surrounded by four nitrogen atoms (N8, N9, N10, and N11) of two phen, three oxygen atoms, O2 and O3 from two water molecules and O4 of an MeOH, and two nitrogen atoms (N2 and N3) of two bridging cyanides. Adjacent Pr^{3+} and Fe^{2+} in $[Pr(phen)_2(MeOH)(H_2O)_2][Fe(CN)_5(NO)]$ are connected by two cynanides (Fe-C1-N2-Pr) and (Fe-C2-N3-Pr) at *trans* positions to give a 1-D zigzag chain along the *b*-axis. The Fe-C bond distance for non-bridged cyanide ions are ~1.939(6) Å while Fe-C distance of a bridged cyanide is 1.950(6) Å, slightly longer, due to better overlapping of the π^* orbital of CN^- with the f-orbital of Pr. The Fe-N1 (nitrosyl) bond distance is 1.623(5) Å and N1–O1 bond distance (nitrosyl) is 1.163(7) Å, equivalent to reported values [26]. The Fe–N1–O1 bond angle of coordinated nitrosyl (NO) is 178.3(7)°. All Pr–N bond distances of

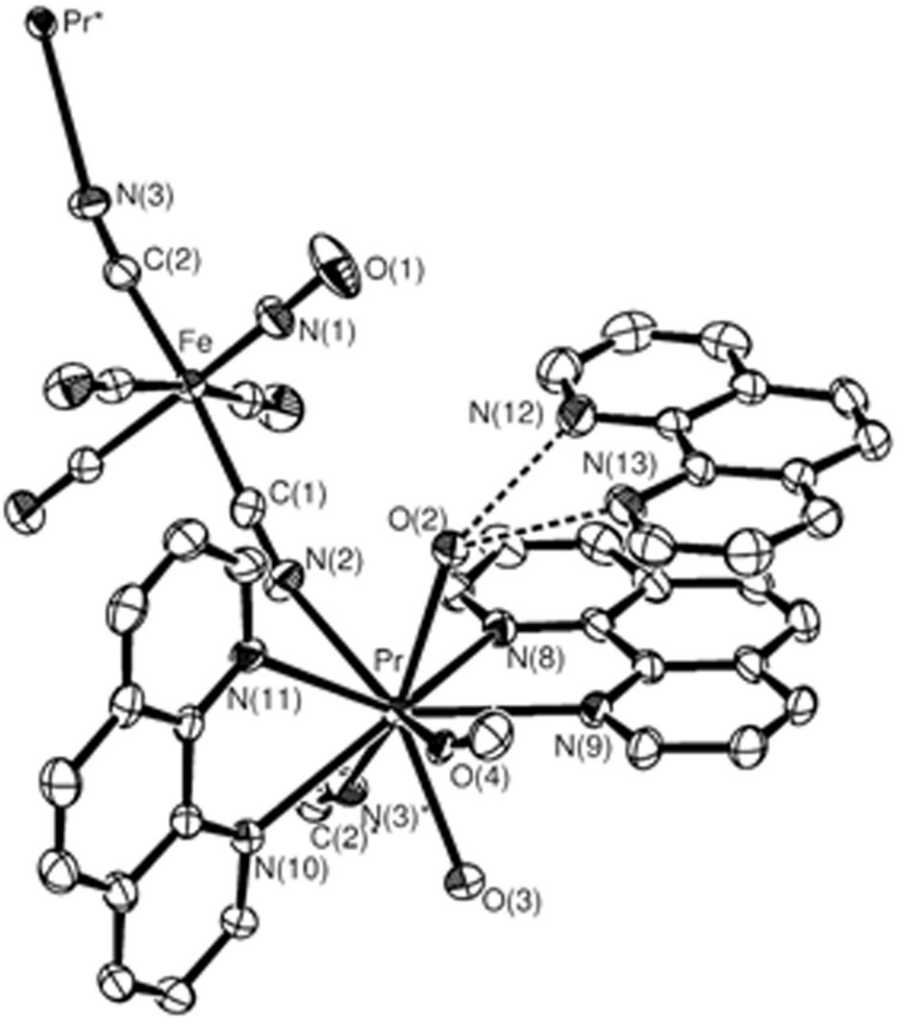

Figure 1. ORTEP of the crystal structure of $[Pr(Phen)_2(MeOH)(H_2O)_2][Fe(CN)_5(NO)]\cdot(Phen)(DMF)(MeOH)(H_2O)$.

coordinated phen are *ca* 2.720(5) Å. The Pr–O2 and Pr–O3 bond distances of coordinated H_2O are 2.502(4) Å and 2.500(4) Å, respectively, while the Pr–O4 distance for coordinated methanol is 2.780(4), slightly longer than that of coordinated H_2O. The Pr-N2 and Pr-N3 bond distances for bridging cyanides are 2.617(5) Å and 2.636(5) Å. The packing diagram of the complex is shown in figure 2. The two nitrogen atoms of an uncoordinated Phen (UC-Phen) form hydrogen bonds with a water molecule in $[Pr(phen)_2(MeOH)(H_2O)_2]^{3+}$ as shown by dotted lines in figure 1. The UC-Phen plays a special role in extending the structure of zigzag chains *via* π–π stacking interactions with the coordinated phen from adjacent chains, so that it forms a sheet structure (figure 2). The distances between the UC- and ligating Phen's, i.e.

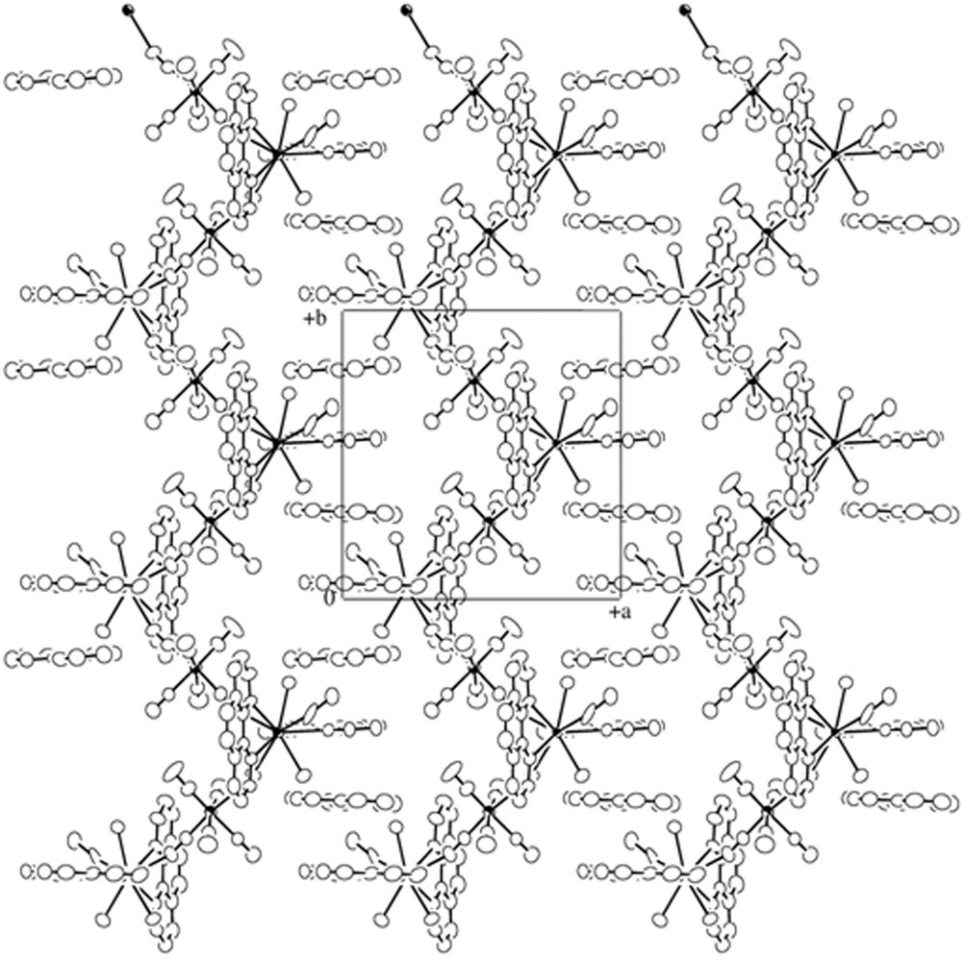

Figure 2. The crystal packing of $[Pr(Phen)_2(MeOH)(H_2O)_2][Fe(CN)_5(NO)]$. The DMF, MeOH, and H_2O molecules are omitted for clarity.

Phen-to-Phen π–π interactions, are 3.35–3.64 Å. The perfect face-to-face π-stacked alignments of the UC- and Phen ligands are clearly favored by dipole–dipole interactions. One DMF is present in the crystal lattice and is linked with coordinated H_2O of $[Pr(phen)_2(MeOH)(H_2O)_2]^{3+}$ through H-bonds at 2.656 Å (O3-H-O5(DMF)).

3.1.2. IR studies. The existence of two types of cyanides in the crystal is supported by IR studies. The absorption at 2152 cm^{-1} can be ascribed as bridging cyanide while the absorption peak at 2131 cm^{-1} is assigned to three terminal cyanides. The νN=O appears at 1918 cm^{-1} [27].

3.1.3. UV-Vis studies. There are two weak bands in the visible region of the spectrum at 446 and 471 nm due to LMCT of $[Fe(NO)(CN)_5]^{3-}$ [28] and one strong band in the ultraviolet region at 324 nm due to π–π^* transition of cyanide and phen in $[Pr(phen)_2(MeOH)(H_2O)_2][Fe(CN)_5(NO)]$.

3.2. *DNA-binding studies*

3.2.1. Electronic spectroscopic studies. Electronic absorption spectroscopy is employed to determine the binding of complexes with DNA. A complex bound to DNA through intercalation is characterized by change in absorbance along with a redshift in wavelength, because of the involvement of a strong stacking interaction between the aromatic chromophore and the DNA base pairs [29–31]. The extent of change of absorption is consistent with the strength of the intercalative interaction. The complex shows two intense absorption bands at 446 nm and 470 nm and two broad bands at 483 nm and 592 nm. The UV-Vis absorption spectrum of the metal complex is significantly modified (figure 3) by the addition of increasing amounts of DNA. In detail, the absorption band at 446 nm is red-shifted by about 5 nm and shows hyperchromism of about 40%. Similar effects are observed in the remaining bands. All these findings support DNA-binding by intercalation through the stacking interaction of the aromatic rings of the ligand and the base pairs of DNA. The intrinsic binding constant K_b was $5.14 \times 10^5 (\text{mol L}^{-1})^{-1}$ (figure 4), comparable to those observed for classical intercalators and metallo-intercalators whose binding constants [32–35] were 10^5–10^7. The observed value of binding constant is also in accord with those of other DNA intercalative lanthanide complexes reported [36–40].

3.2.2. Fluorescence spectroscopic studies. EB is weakly fluorescent, but fluorescence of EB is remarkably enhanced when it is bound to DNA. The emission spectra of the EB-DNA complex in Tris-HCl in the presence of increasing amounts of Pr-phen complex are shown in figure 5. The intensity of fluorescence of EB in the EB-DNA complex is gradually lowered by addition of increasing amounts of Pr-phen complex. This can happen if the complex displaces EB from the DNA cavities. This result confirms that the complex interacts with DNA by an intercalative mechanism [41], thereby competing with EB.

A plot of I_0/I *versus* [complex] is made (figure 6), where I_0 is the fluorescence intensity of EB-DNA control and I is the fluorescence intensity of EB-DNA complex. The results show that the I_0/I value progressively increases with increase in concentration of the complex, suggesting displacement of EB from DNA by the complex and supports our proposition of intercalative binding of DNA by the present compound.

3.2.3. Gel electrophoresis study. The ability of the complex to perform DNA cleavage has been assayed by gel electrophoresis using supercoiled (SC) pUC 19 DNA in Tris-HCl/NaCl buffer (50 mmol L^{-1}, pH 7.2). The complex on reaction with DNA in the presence of H_2O_2 exhibits high nuclease activity (figure 7). Significant cleavage is observed at 1.0×10^{-3} mol L^{-1} and 5.0×10^{-3} mol L^{-1} in the presence of 4 mmol L^{-1} H_2O_2 (table 4). This study shows that the complex cleaves 84% of SC DNA to NC (nicked coiled) DNA. Control experiments show that the cleavage of SC DNA by the

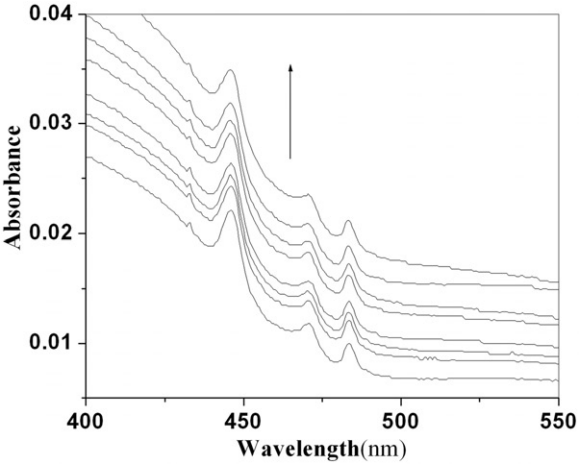

Figure 3. Absorption spectra of Pr-phen complex in the presence of increasing amounts of DNA ([Pr-phen] = 45 μmol L^{-1}, [DNA] = 25–350 μmol L^{-1} from bottom to top). The arrows indicate the change in absorbance upon increasing DNA concentration.

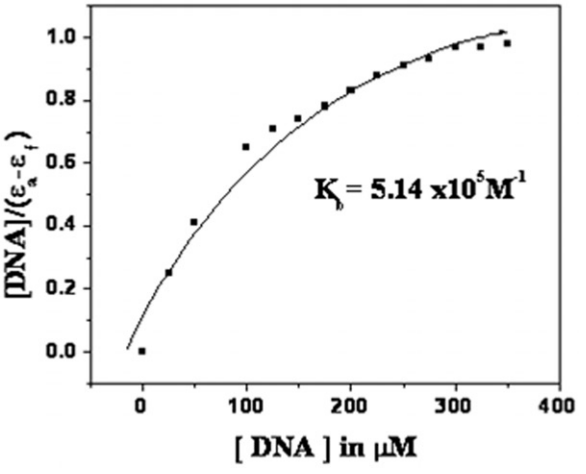

Figure 4. Plots of [DNA]/($\varepsilon_a - \varepsilon_f$) *vs.* [DNA] for the titration of DNA to Pr-phen complex.

complex alone, i.e. in absence of H_2O_2, is negligible. The nuclease mechanism in the presence of H_2O_2 as described elsewhere [18, 42] suggests the possibility of formation of hydroxyl ($HO^{\cdot}$) radicals as the reactive species.

4. Conclusion

The synthesis and structural characterization of a cyano-bridged heterometallic lanthanide transition metal nitrosyl complex, $[Pr(phen)_2(MeOH)(H_2O)_2]$

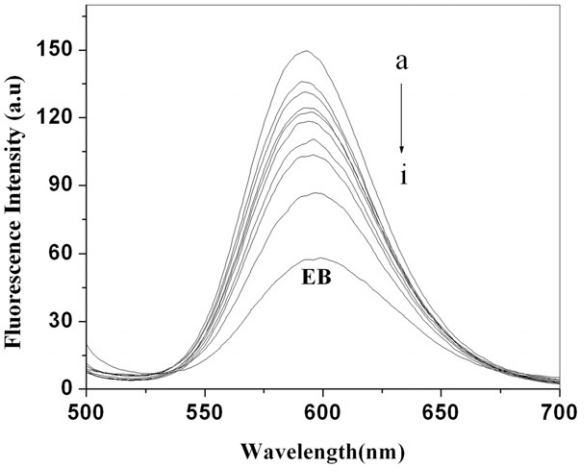

Figure 5. Fluorescence spectra of the EB-DNA complex in the presence of increasing amounts of Pr-phen complex, [EB] = 90.0 μmol L^{-1}, [DNA] = 60.0 μmol L^{-1}: (a) 0.0 μmol L^{-1}, (b) 10.0 μmol L^{-1}, (c) 30.0 μmol L^{-1}, (d) 60.0 μmol L^{-1}, (e) 90.0 μmol L^{-1}, (f) 120 μmol L^{-1}, (g) 150.0 μmol L^{-1}, (h) 180 μmol L^{-1}, and (i) 300.0 μmol L^{-1}.

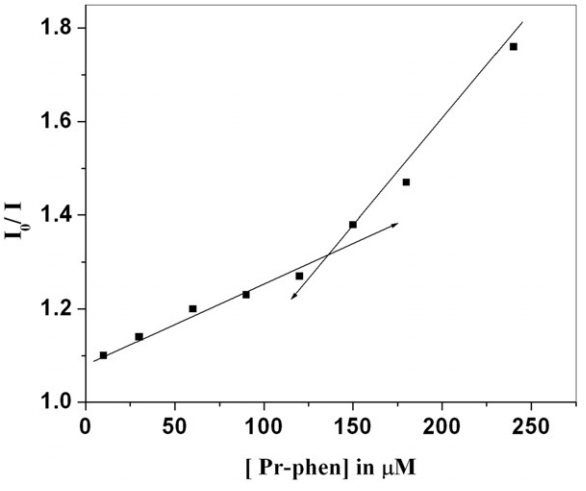

Figure 6. Relative intensity values (I_0/I) at 592 nm of the fluorescence spectra of the EB-DNA complex in the presence of increasing amounts of Pr-phen complex.

$[Fe(CN)_5(NO)] \cdot (Phen)(DMF)(MeOH)(H_2O)$, has been established. Absorption titration studies for DNA-binding by the complex provide $K_b = 5.14 \times 10^5 (mol\,L^{-1})^{-1}$, suggesting that the complex is a good DNA intercalator. Intercalative binding of the complex with DNA has been further supported by fluorimetric studies where the complex competes with EB in binding to DNA. The complex exhibits pronounced nuclease activity in the presence of H_2O_2 on supercoiled (SC) pUC19 DNA.

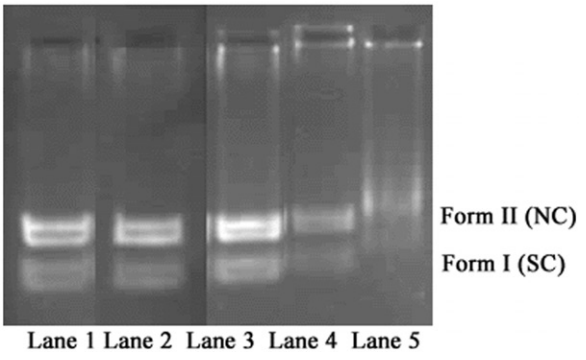

Figure 7. Cleavage of supercoiled pUC19 DNA (0.2 ng) by Pr-phen complex in DMF in the presence of H_2O_2 (4 mmol L^{-1}) in a buffer containing 50 mmol L^{-1} Tris-HCl and 50 mmol L^{-1} NaCl at 37°C. Lane 1, DNA control; Lane 2, DNA + H_2O_2; Lane 3, DNA + 1.0×10^{-3} mol L^{-1} complex; Lane 4, DNA + H_2O_2 + 1.0×10^{-3} mol L^{-1} complex; Lane 5, DNA + H_2O_2 + 5.0×10^{-3} mol L^{-1} complex.

Table 4. Extent of DNA SC pUC19 (0.2 ng) cleavage by the Pr-phen complex.

Sl. No.	Reaction condition	Form I (%SC)	Form II (%NC)
1.	DNA control	75	25
2.	DNA + 4 mmol L^{-1} H_2O_2	70	30
3.	DNA + 1.0×10^{-3} mol L^{-1} complex	65	35
4.	DNA + 4 mmol L^{-1} H_2O_2 + 1.0×10^{-3} mol L^{-1} complex	45	55
5.	DNA + 4 mmol L^{-1} H_2O_2 + 5.0×10^{-3} mol L^{-1} complex	16	84

Supplementary material

Crystallographic data for the structural analysis has been deposited with the Cambridge Crystallographic Data Centre, CCDC No. 283459. Copies of this information may be obtained free of charge from The Director, CCDC, 12 Union Road, Cambridge, CB21EZ, UK (Fax: +441223336033; E-mail: deposit@ccdc.cam.ac.uk or www.ccdc.cam.ac.uk/data_request/cif).

Acknowledgments

The authors are grateful to Jadavpur University for providing facilities and UGC-DAE-CSR, KC (Ref.No.-CRS/09/RC03/1456), India for funding in the form of a major research project to KKM.

References

[1] G.B. Richter-Addo, R. Legzdins, P. Burstyn. *Chem. Rev.*, **102**, 857 (2002).
[2] T.W. Hayton, P. Legzdins, W.B. Sharp. *Chem. Rev.*, **102**, 935 (2002).

[3] M. Madhani, A.K. Patra, T.W. Miller, A.A. Eroy-Reveles, A.J. Hobbs, J.M. Fukuto, P.K. Mascharak. *J. Med. Chem.*, **49**, 7325 (2006).
[4] U. Schatzschneider. *Eur. J. Inorg. Chem.*, 1451 (2010).
[5] J.A. McCleverty, M.D. Ward. *Compr. Coord. Chem.*, **2**, 743 (2004).
[6] P.L. Feldman, O.W. Griffith, D.J. Stuehr. *Chem. Eng. News*, **20**, 26 (1993).
[7] J.S. Stamler, D.J. Singel, D.J. Loscalzo. *Science*, **258**, 1898 (1992).
[8] A.R. Butler, D.L.H. Williams. *Chem. Soc. Rev.*, **22**, 233 (1993).
[9] P.G. Baraldi, M.A. Tabrizi, D. Preti, F. Fruttarolo, B. Avitabile, A. Bovero, G. Pavani, M.C.N. Carretero, R. Romagnoli. *Pure Appl. Chem.*, **75**, 187 (2003).
[10] S. Ramakrishnan, V. Rajendiran, M. Palaniandavar, V.S. Periasamy, B.S. Srinag, H. Krishnamurthy, M.A. Akbarsha. *Inorg. Chem.*, **48**, 1309 (2009).
[11] P.G. Sammes, G. Yahioglu. *Chem. Soc. Rev.*, **23**, 327 (1994).
[12] Y. Sun, S.N. Collins, L.E. Joyce, C. Turro. *Inorg. Chem.*, **49**, 4257 (2010).
[13] J.K. Barton. *Science*, **233**, 727 (1986).
[14] K. Midorikawa, M. Murata, S. Oikawa, S. Tada-Oikawa, S. Kawanishi. *Chem. Res. Toxicol.*, **13**, 309 (2000).
[15] M. Sam, J.H. Hwang, G. Chanfreau, M.M. Abu-Omar. *Inorg. Chem.*, **43**, 8447 (2004).
[16] O. Zelenko, J. Gallagher, Y. Xu, D.S. Sigman. *Inorg. Chem.*, **37**, 2198 (1998).
[17] T.K. Si, S.S. Paul, K.K. Mukherjea. *Dalton Trans.*, **41**, 5805 (2012).
[18] M. Selim, K.K. Mukherjea. *J. Biomol. Struct. Dyn.*, **26**, 561 (2009).
[19] M. Selim, S.R. Chowdhury, K.K. Mukherjea. *Int. J. Biol. Macromol.*, **41**, 579 (2007).
[20] D.D. Perrin, W.L.F. Armarego, D.R. Perrin. *Purification of Laboratory Chemicals*, Pergamon Press, New York (1966).
[21] J. Marmur. *J. Mol. Biol.*, **3**, 208 (1961).
[22] M.F. Reichmann, S.A. Rice, C.A. Thomas, P. Doty. *J. Am. Chem. Soc.*, **76**, 3047 (1954).
[23] Bruker Advanced X-ray Solutions. *SAINT (Version 6.02), SADABS (Version 2.03)*, Bruker AXS Inc., Madison, WI, USA (2002).
[24] G.M. Sheldrick. *SHELXL-97, Program for X-ray Crystal Structure Refinement*, University of Gottingen, Germany (1997).
[25] A. Wolfe, G.H. Shimer, T. Meehan. *Biochem.*, **26**, 6392 (1987).
[26] H.W. Chen, C.W. Lin, C.C. Chen, L.B. Yang, M.H. Chiang, W.F. Liaw. *Inorg. Chem.*, **44**, 3226 (2005).
[27] S.W. Liang, M.X. Li, M. Shao, H.J. Liu. *J. Mol. Struct.*, **841**, 73 (2007).
[28] P.T. Manoharan, H.B. Gray. *J. Am. Chem. Soc.*, **5**, 3340 (1965).
[29] J.K. Barton, A.T. Danishefsky, J.M. Goldberg. *J. Am. Chem. Soc.*, **106**, 2172 (1984).
[30] S.A. Tysoe, R.J. Morgan, A.D. Baker, T.C. Strekas. *J. Phys. Chem.*, **97**, 1707 (1993).
[31] T.M. Kelly, A.B. Tossi, D.J. McConnell, T.C. Strekas. *Nucleic Acids Res.*, **13**, 6017 (1985).
[32] G. Zhao, F. Li, H. Lin, H. Lin. *Bioorg. Med. Chem.*, **15**, 533 (2007).
[33] B. Peng, H. Chao, B. Sun, H. Li, F. Gao, L.N. Ji. *J. Inorg. Biochem.*, **101**, 404 (2007).
[34] A. Silvestri, G. Barone, G. Ruisi, D. Anselmo, S. Riela, V.T. Liveri. *J. Inorg. Biochem.*, **101**, 841 (2007).
[35] B. Macýas, I. Garcýa, M.V. Villa, J. Borras, M.G. Alvarez, A. Castineiras. *J. Inorg. Biochem.*, **96**, 367 (2003).
[36] Z.H. Xu, P.X. Xi, F.J. Chen, Z.Z. Zeng. *J. Coord. Chem.*, **62**, 2193 (2009).
[37] H.-Z. Pan, X.-M. Wang, H.-B. Li, Q. Yang, L.-S. Ding. *J. Coord. Chem.*, **63**, 4347 (2010).
[38] Y. Li, Z. Yang. *J. Coord. Chem.*, **63**, 1960 (2010).
[39] J. Huang, X. Wang, L. Ding. *J. Coord. Chem.*, **64**, 2791 (2011).
[40] M. Wang, Z. Yang, Y. Li, H. Li. *J. Coord. Chem.*, **64**, 2974 (2011).
[41] G.D. Liu, J.P. Liao, S.S. Huang, G.L. Shen, R.Q. Yu. *Anal. Sci.*, **17**, 1031 (2001).
[42] C. Liu, S. Yu, D. Li, Z. Liao, X. Sun, H. Xu. *Inorg. Chem.*, **41**, 913 (2002).